THE JOURNAL OF PHYSICAL CHEMISTRY C
A JOURNAL OF THE AMERICAN CHEMICAL SOCIETY

pubs.acs.org/JPCC

Article

Effect of Calcium on the Atomic and Electronic Structures of CdSe QD-Embedded Soda–Lime–Silica Glasses

Wenke Li, Xiujian Zhao, François-Xavier Coudert,* and Chao Liu*

Cite This: *J. Phys. Chem. C* 2022, 126, 14283–14289

Read Online

ACCESS | Metrics & More | Article Recommendations | Supporting Information

ABSTRACT: In this work, we have investigated the effects of calcium on the atomic and electronic structures of CdSe quantum dots (QDs) by *ab initio* molecular dynamics. The increase in the CaO content in glass is found to break the linkage between Na and O atoms, while interactions between Cd atoms and nonbridging oxygen atoms are not disrupted. The presence of the CdSe QDs promotes the migration of Na atoms from the glass matrix to the interface and even the interior of CdSe QDs, while Ca atoms are only found to be present at the QD/glass interface and in glass matrices far from the QDs. However, on the basis of the radial concentration distribution, the CdSe QD only impacts the structure of glass at a short range near the interface. The increase in the CaO content is also shown to increase the highest occupied molecular orbital–lowest unoccupied molecular orbital (HOMO–LUMO) gap of CdSe QD-embedded glasses. Our findings can extend the understanding of the effects of calcium on the structural and luminescence properties of CdSe QD-embedded glasses.

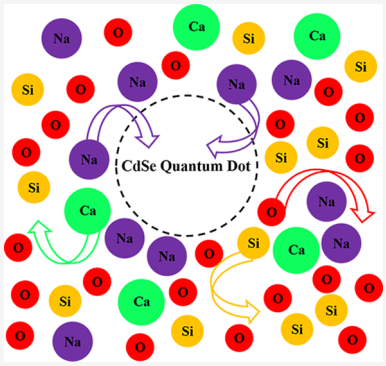

1. INTRODUCTION

Quantum dots (QDs) have stimulated large research interest because of their size-tunable optical and electronic properties. Their appealing properties include narrow emission linewidth and high quantum yields, making them near-ideal nanomaterials for energy conversion and lighting technologies.[1,2] Compared to colloidal QDs, QD-embedded glasses can combine the excellent thermal, mechanical, and chemical stability of the glass matrix and the remarkable optical properties of QDs. Therefore, QD-embedded glasses have great potentials for applications in the field of light-emitting diodes (LEDs),[3,4] lasers,[5] and solar converters.[6] The emission of CdSe QDs covering the entire visible spectral range by controlling the size of nanocrystals has been extensively studied.[7−10]

However, the practical application of CdSe QD-embedded glasses suffers from their very low quantum yields compared with their colloidal counterparts. It has been proposed that the defects on the interface between QDs and the glass matrix are detrimental to the excitonic emission, resulting in the commonly observed defect emission.[11] However, origins of the defects have not been clarified so far, which is mainly caused by the difficulty to probe the interfacial atomic structure between CdSe QDs and the glass matrix, due to the low concentration of CdSe QDs, the insulating nature of glass, and the instability of glass under intense electron beam irradiation. Computational simulations provide an alternative to obtain insights into this issue, by investigating a system at the atomistic level, which is not directly accessible in experiments. The atomic[12] and electronic structures[13] of CdSe QD-embedded binary sodium silicate glasses have been explored in our previous studies based on the *ab initio* molecular dynamics. Breakages of CdSe coordination have been found at both the QD/glass interface and in the core of the CdSe QDs, with the formation of Se–Na and Cd–O bonds at the interface. The strong reconstruction of CdSe QDs also contributed to changes in their electronic structures. The nature of the highest occupied molecular orbital (HOMO) was determined by oxygen atoms in some glasses, while it was decided by Se atoms in glasses with different Na_2O/SiO_2 ratios. Therefore, the composition of glasses plays a significant role in the atomic and electronic structures of CdSe QDs.

In our previous study, the investigated glass was limited to sodium silicate glass composed of Na_2O and SiO_2, while the experimentally fabricated glasses were usually multicomponent. The soda–lime–silica system forms the basis for a wide range of commercially important glass products. These compositions are commonly used for the CdSe QD-embedded glasses, although usually, additional minor components are present. Therefore, the effect of calcium on the atomic and electronic structures of CdSe QD-embedded glasses is supposed to be investigated. In this paper, we report the results of an *ab initio* molecular dynamics study of CdSe QDs embedded in a $(25 - x)\ Na_2O - x\ CaO - 75\ SiO_2$ (x = 5, 10, 15, in mol %) system. The Se–Na, Se–Ca, and Cd–O bonds are observed at the

Received: June 6, 2022
Revised: July 15, 2022
Published: August 11, 2022

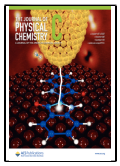

https://doi.org/10.1021/acs.jpcc.2c03917
J. Phys. Chem. C 2022, 126, 14283–14289

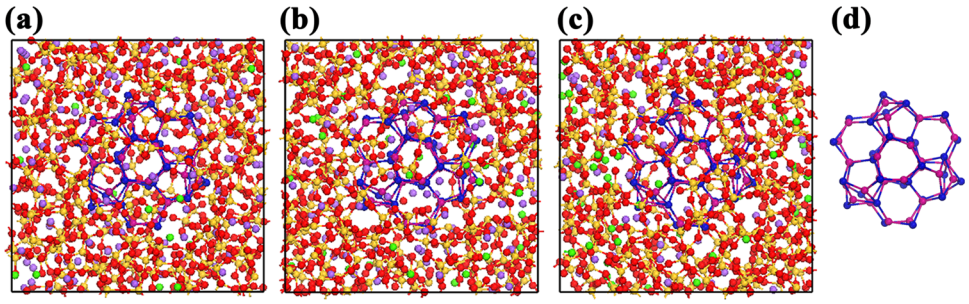

Figure 1. Initial structures of classical molecular dynamics. Glass composition: (a) x = 5:68 Na_2O-17 CaO-255 SiO_2-33 CdSe, (b) x = 10:51 Na_2O-34 CaO-255 SiO_2-33 CdSe, and (c) x = 15:34 Na_2O-51 CaO-300 SiO_2-33 CdSe and (d) pristine QDs. The color codes of the atoms are magenta for Cd, blue for Se, purple for Na, green for Ca, red for O, and yellow for Si.

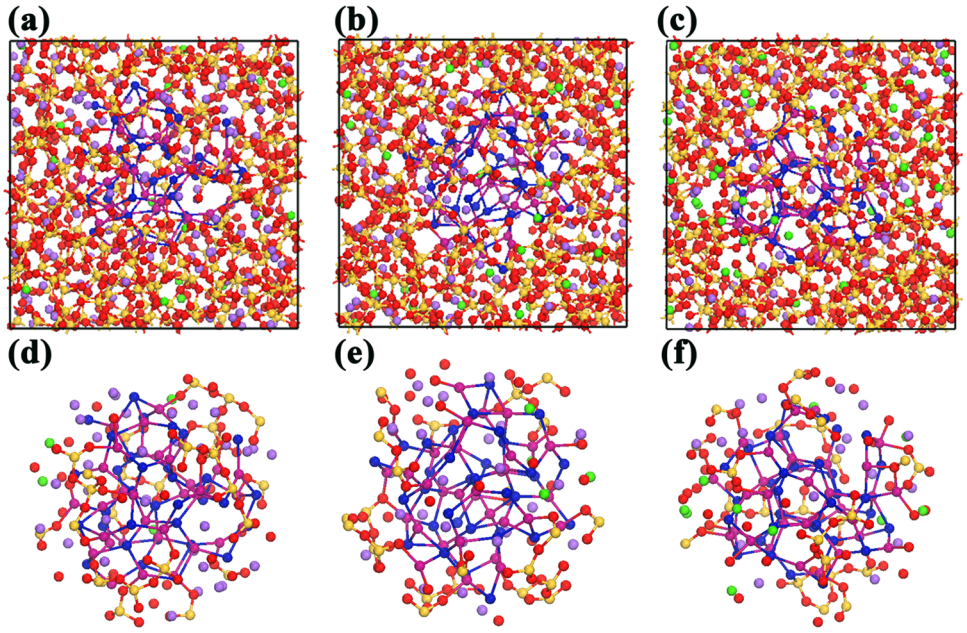

Figure 2. Final structures from the *ab initio* molecular dynamics simulations. Glass composition: (a) x = 5:68 Na_2O-17 CaO-255 SiO_2-33 CdSe, (b) x = 10:51 Na_2O-34 CaO-255 SiO_2-33 CdSe, and (c) x = 15:34 Na_2O-51 CaO-300 SiO_2-33 CdSe. (d)−(f) Partial enlargement of the final structure corresponding to (a)−(c), respectively.

QD/glass interface based on the analysis of the radial distribution function (RDF). The increase in the CaO content enhances the stability of CdSe QDs but weakens the interaction between O and Na atoms. The existence of CdSe QDs leads to the migration of Na atoms from glass matrices to the interface and the interior of CdSe QDs, while contributing to the migration of O atoms and Si atoms from the interface to the glass matrices. Ca atoms only exist in the interface of QD/glass and in regions far from the QD. The effects of CdSe QDs on the glass structure are only observed in a short range according to the analysis of the radial concentration distribution. With the additional introduction of the CaO content, the highest occupied molecular orbital−lowest unoccupied molecular orbital (HOMO−LUMO) gap is found to increase, and all the frontier orbitals are decided by hybrid QDs.

2. COMPUTATIONAL METHODS

The methodology used here to generate QD/glass models was developed and validated in our previous work, and it is based on a combination of classical and *ab initio* molecular dynamics.[12] First, atoms were randomly placed in a cubic simulation box using the Packmol code,[14] generating an initial configuration of the glass matrix. The total number of atoms in the glass matrix was 1180, 1160, and 1140, with the simulation sizes of 25.340, 25.227, and 25.112 Å, respectively. Compositions of these glasses are 80 Na_2O-40 CaO-300 SiO_2, 60 Na_2O-40 CaO-300 SiO_2, and 40 Na_2O-60 CaO-300 SiO_2. From this initial configuration, the glass structures were generated using a melt quenching approach ranging from 6000 to 300 K, in the (N, V, T) ensemble at the target density,[15] with a partially charged rigid-ion pairwise potential.[16] The molecular dynamics simulations were run using the DL_POLY package.[17] The Coulomb interactions were calculated using the Ewald summation method with a precision of 10^{-5} and the real-space cutoff for short-range interactions set to 7.6 Å.

Second, the $Cd_{33}Se_{33}$ QD structure obtained at the density functional theory (DFT) level in a previous study[18] was incorporated into this glass matrix, removing glass atoms, so the interatomic distance between the QD and glass matrix was longer than 2.5 Å. The final composition was 68 Na_2O-17 CaO-255 SiO_2-33 CdSe (x = 5), 51 Na_2O-34 CaO-255 SiO_2-33 CdSe (x = 10), and 34 Na_2O-51 CaO-300 SiO_2-33 CdSe (x = 15) (Figure 1).The interaction between Cd and Se atoms

https://doi.org/10.1021/acs.jpcc.2c03917
J. Phys. Chem. C 2022, 126, 14283−14289

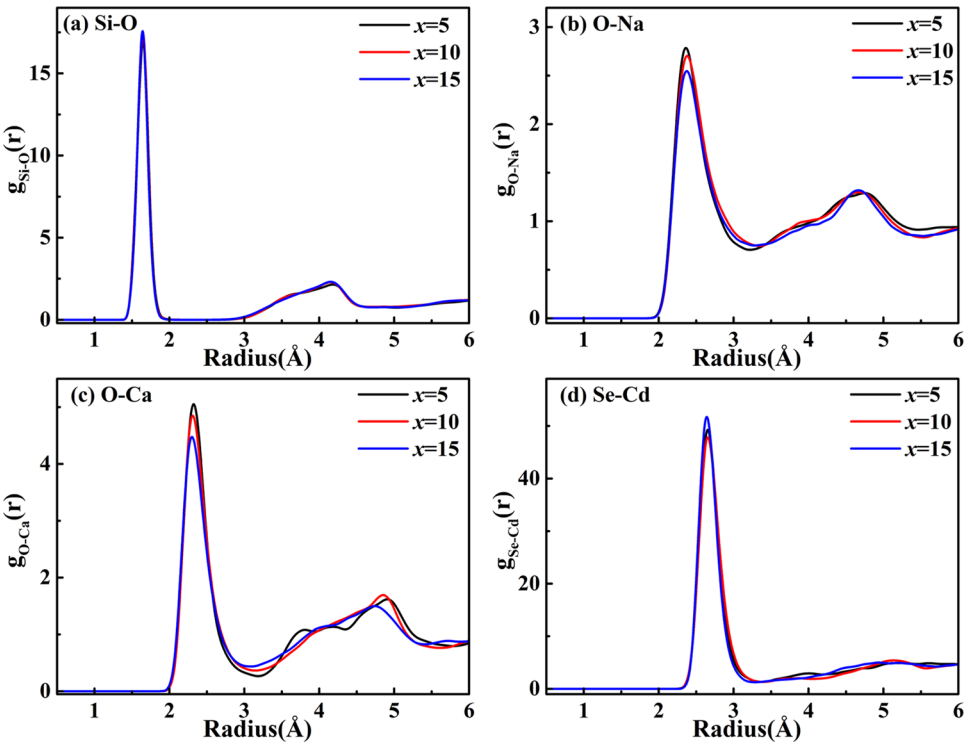

Figure 3. Radial distribution functions for (a) Si−O, (b) O−Na, (c) O−Ca, and (d) Se−Cd pairs, averaged over the ab initio molecular dynamics trajectories for CdSe QDs embedded in $(25 - x)$ Na_2O-x CaO-75 SiO_2 glasses. The black, red, and blue lines represent the glass composition with x equal to 5, 10, and 15, respectively.

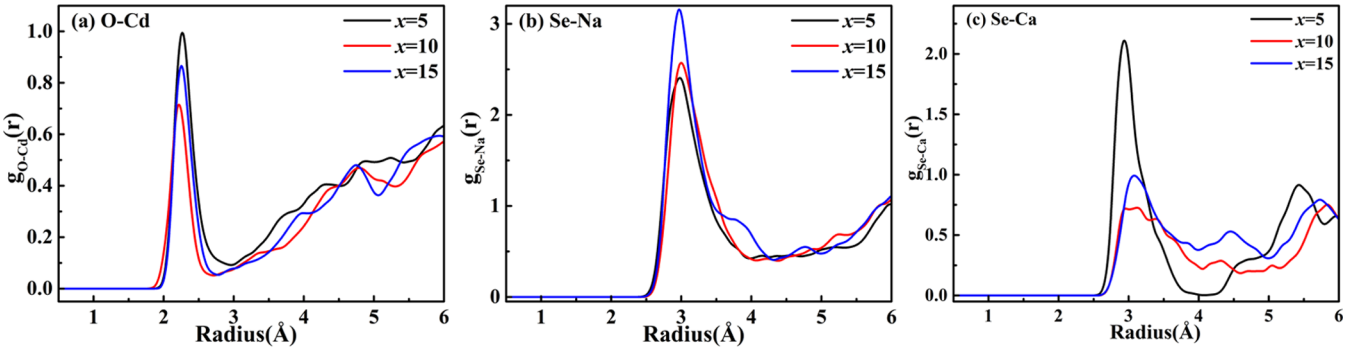

Figure 4. Radial distribution functions for (a) O−Cd, (b) Se−Na, and (c) Se−Ca pairs, averaged over the ab initio molecular dynamics trajectories for CdSe QDs embedded in $(25 - x)$ Na_2O-x CaO-75 SiO_2 glasses. The black, red, and blue lines represent the glass composition with x equal to 5, 10, and 15, respectively.

was described by a Lennard−Jones pairwise potential,[19] while the Lorentz−Berthelot combining rules were used for interactions between the glass matrix and QD. After equilibrating at 1000 K with 200 ps NVT and 200 ps NVE dynamics, the whole structures were quenched from 1000 to 500 K in steps of 50 K, keeping the CdSe QDs frozen. Then, they were gradually cooled from 500 to 300 K in steps of 10 K, with all atoms allowed to move. The structures were further equilibrated at 300 K with 200 ps NVT and NVE dynamics.

Finally, after equilibrating the systems using the classical molecular dynamics described above, the resulting structures were employed as the initial configurations for *ab initio* molecular dynamics, with interatomic forces calculated at the density functional theory (DFT) level, using the CP2K code.[20] The Perdew−Burke−Ernzerhof (PBE) exchange−correlation function was used.[21] For Na, Ca, Cd, and Se, we used short-range molecularly optimized double-ζ single-polarized basis sets (DZVP-MOLOPT-SR-GTH), while for O and Si, we used a double-ζ single-polarized basis set (DZVP-MOLOPT-GTH).[22] The plane wave cutoff and relative cutoff were set to 600 Ry and 40 Ry, respectively. The structure was quenched from 500 to 300 K in steps of 50 K, with a 10 ps *ab initio* molecular dynamics run at a time step of 2 fs. The production run was conducted in the NVT ensemble at 300 K for 10 ps.

For each system, 500 configurations were selected at equal intervals from a 10 ps production run of *ab initio* molecular dynamics simulations. Among these, 50 configurations were picked to perform the calculation and analysis of the electronic structure of CdSe QD-embedded glasses. We used the nonlocal PBE0-TC-LRC[23] exchange−correlation functional with a cutoff radius of 4.0 Å. Moreover, the computational cost of nonlocal functional calculations can be reduced using the auxiliary density matrix method (ADMM).[24]

https://doi.org/10.1021/acs.jpcc.2c03917
J. Phys. Chem. C 2022, 126, 14283−14289

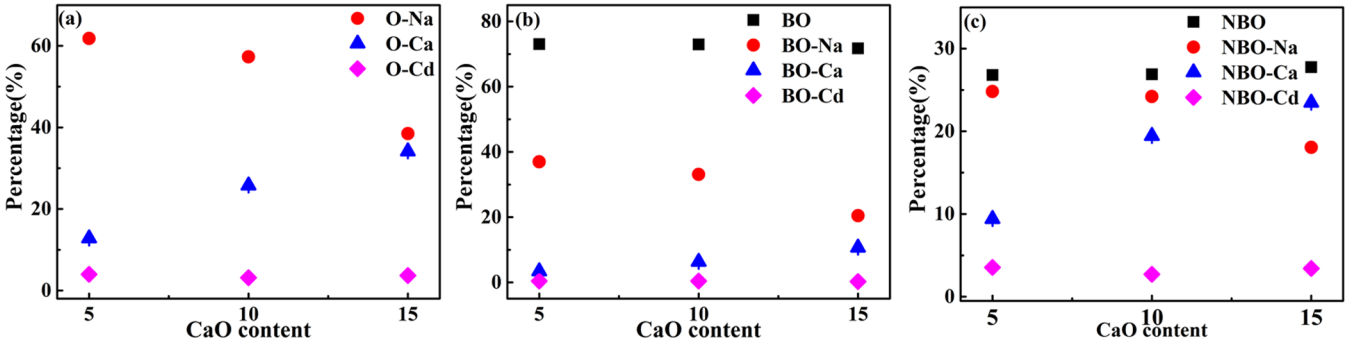

Figure 5. 500 configurations obtained by a 10 ps production run were divided into 5 blocks and the coordination environment of O atoms was analyzed for each block. The error bars represent standard deviation. (a) Ratio between the number of oxygen atoms coordinated with Na atoms, Ca atoms, or Cd atoms and the total number of oxygen atoms. (b) Ratio between the number of bridging oxygen atoms (BO), BO coordinated with Na atoms, BO coordinated with Ca atoms, or BO coordinated with Cd atoms and the total number of oxygen atoms. (c) Ratio between the number of nonbridging oxygen atoms (NBO), NBO coordinated with Na atoms, NBO coordinated with Ca atoms, or NBO coordinated with Cd atoms and the total number of oxygen atoms.

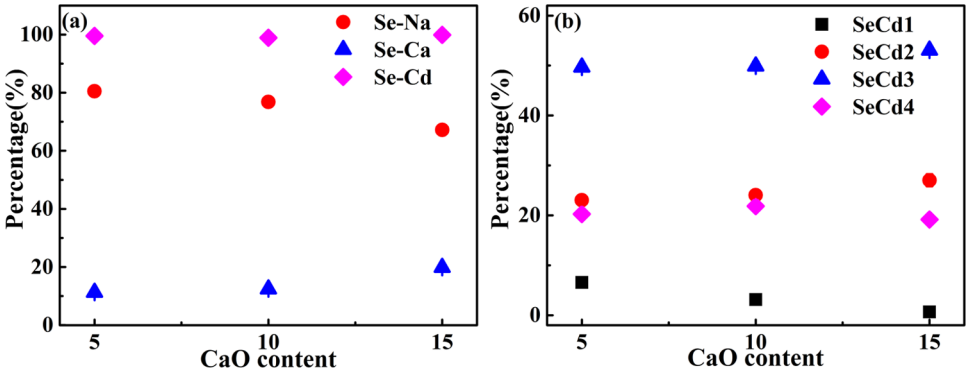

Figure 6. 500 configurations obtained by a 10 ps production run were divided into 5 blocks and the coordination environment of Se atoms was analyzed for each block. The error bars represent standard deviation. (a) Ratio between the number of Se atoms coordinated with Na atoms, Ca atoms, or Cd atoms and the total number of Se atoms. (b) Ratio between the number of Se atoms 1-coordinated, 2-coordinated, 3-coordinated, or 4-coordinated with Cd atoms and the total number of Se atoms.

3. RESULTS AND DISCUSSION

The final configurations of the *ab initio* simulations are shown in Figure 2. Compared to the pristine CdSe QDs in the initial structure (Figure 1d), we see that the CdSe QDs undergo a strong structural reconstruction, similar in nature to what was previously observed in other QD/glass systems.[12,13] In pristine QDs, Cd atoms (Se atoms) are 3-coordinated with Se atoms (Cd atoms) on the surface, while Cd atoms (Se atoms) are 4-coordinated with Cd atoms (Se atoms) in the core. For the CdSe QDs in glass matrices, breakage of stable 6-membered Cd-Se rings is observed with the formation of 1- or 2-coordinated Cd atoms or Se atoms at the interface. It is hard for the CdSe QD to maintain its bulk structure even in the core.

Based on the analysis of radial distribution function (RDF) obtained over the *ab initio* molecular dynamics, the first-neighbor peaks for Si−O (Figure 3a), O−Na (Figure 3b), O−Ca (Figure 3c), and Se−Cd (Figure 3d) pairs are found at 1.64, 2.36, 2.27, and 2.63 Å, respectively, consistent with the experimental and theoretical values.[19,25] Looking into the QD/glass interface, the formation of O−Cd, Se−Na, and Se−Ca bonds observed visually is confirmed by the analysis of RDF for these pairs (Figure 4). Although there are some fluctuations of the interatomic distance of each pair in different glass compositions, the first-neighbor peak is located near 2.25 Å (Figure 4a), 2.98 Å (Figure 4b), and 3.00 Å (Figure 4c) for O−Cd, Se−Na, and Se−Ca, respectively. The interatomic distances for Cd−O bonds were found to be 2.25 Å based on the extended X-ray absorption fine structure spectroscopy (EXAFS) analysis of CdSe QD-embedded glasses.[26] The Se−Na and Se−Ca distances observed in the heavier alkaline earth complexes with phosphinoselenoic amides were 3.01 and 2.99 Å, respectively (characterized by single-crystal X-ray diffraction).[27]

Furthermore, we explored the coordination environment of oxygen atoms (Figure 5). With the increase of the CaO content in the glass, we observe that the ratio between the number of O atoms coordinated with Na atoms and the total number of O atoms decreases, while that of O atoms coordinated with Ca atoms increases. However, the ratio between the number of O atoms bonded with Cd atoms and the total number of oxygen atoms only slightly fluctuates with the increase of the CaO content (Figure 5a). To get a deeper insight into this coordination, we divide oxygen atoms into two groups: nonbridging oxygen atoms (NBO) and bridging oxygen atoms (BO). The ratio between the number of BO and oxygen atoms is estimated to be 83.5% based on the ratio between glass modifiers and glass formers, which is slightly higher than the 73.0% in our model due to the presence of CdSe QDs (Figure 5b). It is visible that calcium ions compete with sodium ions to coordinate with BO and NBO (Figure 5c). Additionally, BO are more likely to be surrounded with

https://doi.org/10.1021/acs.jpcc.2c03917
J. Phys. Chem. C 2022, 126, 14283−14289

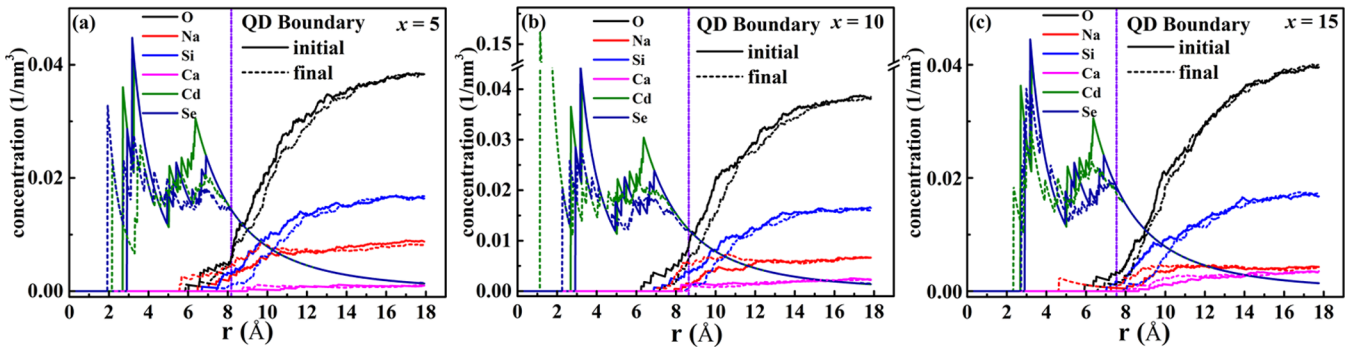

Figure 7. Radial concentration distribution of O atoms (black line), Na atoms (red line), Si atoms (blue line), Ca atoms (magenta line), Cd atoms (green line), and Se atoms (navy line) of the initial configuration of classical molecular dynamics (solid line) and the final configuration (dash line) obtained by *ab initio* molecular dynamics. Glass composition: (a) $x = 5$, (b) $x = 10$, and (c) $x = 15$. The origin is the geometric center, and the QD boundary (purple vertical dash line) is the most external region of the CdSe QD.

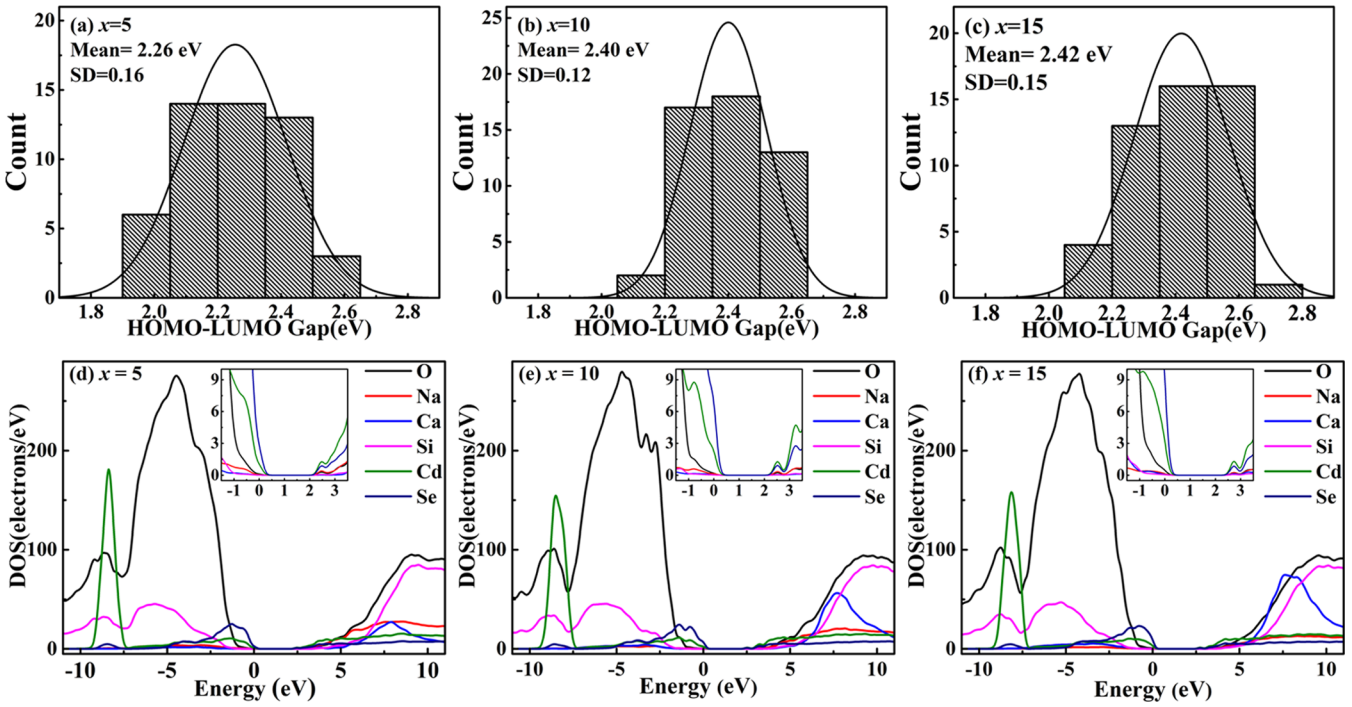

Figure 8. HOMO−LUMO gap distribution of 50 configurations of the *ab initio* molecular dynamics production run of glasses with x equal to (a) 5, (b) 10, and (c) 15. (d) Density of states of the final configuration from the *ab initio* molecular dynamics production run. (e, f) Composition of x = 5, 10, and 15, respectively.

Na ions, while Ca ions are favored by NBO, consistent with previous studies.[15,28,29] Almost all Cd ions interact with NBO rather than with BO, and these interactions are not impacted by the increase of the CaO content. These trends can be explained by the single-bond strength of each pair. The nondirectional ionic Na−O bonds are weaker than the Ca−O bonds due to the high field strength of Ca atoms with higher valence and smaller radius. However, the external shell of Cd^{2+} contains 18 electrons, resulting in strong polarization of oxygen atoms. Therefore, the single-bond strength of each pair increases in the order of O−Na, O−Ca, and O−Cd.

The coordination environment of Se atoms in the different systems was also investigated. All the Se atoms are bonded with Cd atoms, while the Na atoms tend to bond preferentially with Se atoms than with Ca atoms (Figure 6a). The percentage of Se atoms coordinated with Na atoms decreases from 80.50 and 76.81 to 67.21% with the increase of the CaO content, while the percentage of Se atoms interacting with Ca atoms increases from 11.25 and 12.44 to 19.83%. In the initial configuration (Figure 1), 63.64% of the Se atoms are 3-coordinated with Cd atoms and 36.36% of the Se atoms are 4-coordinated with Cd atoms. Stable $SeCd_3$ and $SeCd_4$ units are observed, replaced by the formation of unstable $SeCd_2$ and $SeCd_1$ units (Figure 6b). Meanwhile, it is apparent that the stability of CdSe QDs improved with the addition of CaO, consistent with the final geometrical structure shown.

An additional observation is that the Ca atoms tend to distribute on the spatial region far from the CdSe QDs (Figure 2). Therefore, the radial concentration distribution of each element was calculated (Figure 7). Taking the geometric center of CdSe QDs as the origin, the radial concentrations are calculated as the ratio between the number of atoms of each element and the volume of ball with radius r. The QD boundary is defined as the most external region of CdSe QDs.

https://doi.org/10.1021/acs.jpcc.2c03917
J. Phys. Chem. C 2022, 126, 14283−14289

Compared with the initial structure, the concentrations of O atoms and Si atoms are lower within the QD boundary, demonstrating that the O atoms and Si atoms are more likely to distribute far from the QD region. However, an opposite trend is observed with the concentration of Na atoms within the QD boundary higher than that of the initial structure. Moreover, no Ca atoms are found in the interior of the CdSe QDs. We can draw a conclusion that the existence of CdSe QDs terminates the Si−O network at the interface and promotes the migration of Na atoms from glass matrices to the interior of CdSe QDs. The migration of Ca atoms is complex. The radial concentration profile near the CdSe QD of the final configuration is slightly higher than that of the initial configuration with the composition of x equal to 5 and 15, while it is slightly smaller than that of the initial structure with x = 10. Due to the high field strength and high coordination number between Ca atoms and O atoms, Ca atoms are hard to move in glass matrices. It should be noted that the concentration of each element is equal to that of the initial structure at r = 14 Å, reflecting that the presence of CdSe QDs can only have an impact in the short-range scale and the glass matrices far from the QDs can keep their pristine status. We also calculated the radial concentration of 500 configurations and took an average. The results shown in Figure 1 are consistent with the findings described above.

The electronic structure was also studied to probe the impact of calcium. The average HOMO−LUMO gap increases from 2.26 and 2.40 to 2.42 eV when x changes from 5 to 15 (Figure 8a−c). Therefore, addition of the CaO content in glass matrices can increase the HOMO−LUMO gap of CdSe QD-embedded glasses. According to the radial concentration distribution, the CdSe QD-embedded glasses can be spatially divided into three parts: hybrid QD, hybrid glass, and pristine glass. Strong structural reconstruction happens in CdSe QDs, resulting in a geometrical structure different from that of pristine QDs, which we termed hybrid QDs here. Meanwhile, the existence of CdSe also contributes to the rearrangement of the atomic structure of glasses, leading to the formation of hybrid glass near the QD/glass interface, while the structure of glass far from CdSe QDs keeps the pristine status. The density of states of 50 configurations selected from the AIMD production run was calculated, and similar conclusions can be drawn. Based on the analysis of density of states, the HOMO and LUMO are decided by the Se and Cd atoms, respectively. Therefore, the frontier orbitals are entirely determined by the hybrid QDs. This finding is different from that of our previous work,[13] while the HOMO was determined by hybrid glasses with the glass matrix composition of 33 Na_2O−67 SiO_2. Therefore, calcium also plays a different role in determining the electronic structure of CdSe QD-embedded glasses.

4. CONCLUSIONS

In this work, we have investigated the effects of calcium ions on the atomic and electronic structures of CdSe QD-embedded soda−lime−silica glasses by *ab initio* molecular dynamics. The Se−Na, Se−Ca, and Cd−O coordination is observed at the QD/glass interface with breakage of stable 6-membered Cd−Se rings within the QD. With the increase of the CaO content in the surrounding glass matrices, the stability of the CdSe QD is enhanced. Based on the analysis of the coordination environment of oxygen atoms, the interaction between NBO and Na atoms is weakened, while the interaction between NBO and Cd atoms is not impacted, upon the increase of the CaO concentration. On the other hand, Se atoms are more likely to bond with Na atoms than with Ca atoms. According to the analysis of the radial concentration distribution, although both Na and Ca atoms are glass modifiers, they exhibit different behaviors in our molecular dynamics simulations. The Na atoms tend to migrate from the glass matrix toward the interface, even in the interior of CdSe QDs, while Ca atoms only localize at the interface. The presence of the CdSe QDs in the glasses also promotes the migration of O atoms and Si atoms from the interface into the glass matrices. Meanwhile, we see that the presence of the CdSe QDs only affects the short-range atomic structure of glasses at the interface, and the glass far from the CdSe QDs can maintain its pristine status. The HOMO−LUMO gap increases with the additional introduction of CaO contents in the glass matrix, and the frontier orbitals are both determined by the hybrid QD.

■ ASSOCIATED CONTENT

Supporting Information

The Supporting Information is available free of charge at https://pubs.acs.org/doi/10.1021/acs.jpcc.2c03917.

Radial concentration distributions averaged over the *ab initio* molecular dynamics trajectory (PDF)

■ AUTHOR INFORMATION

Corresponding Authors

François-Xavier Coudert − *Chimie ParisTech, PSL University, CNRS, Institut de Recherche de Chimie Paris, 75005 Paris, France;* orcid.org/0000-0001-5318-3910; Email: fx.coudert@chimieparistech.psl.eu

Chao Liu − *State Key Laboratory of Silicate Materials for Architectures, Wuhan University of Technology, 430070 Hubei, China;* orcid.org/0000-0003-4324-6409; Email: hite@whut.edu.cn

Authors

Wenke Li − *State Key Laboratory of Silicate Materials for Architectures, Wuhan University of Technology, 430070 Hubei, China; Chimie ParisTech, PSL University, CNRS, Institut de Recherche de Chimie Paris, 75005 Paris, France;* orcid.org/0000-0001-9018-7769

Xiujian Zhao − *State Key Laboratory of Silicate Materials for Architectures, Wuhan University of Technology, 430070 Hubei, China;* orcid.org/0000-0002-2517-2605

Complete contact information is available at: https://pubs.acs.org/10.1021/acs.jpcc.2c03917

Notes

The authors declare no competing financial interest.

■ ACKNOWLEDGMENTS

This work was financially supported by the National Natural Science Foundation of China (grant no. 62175192). The authors acknowledge the access to high-performance computing platforms provided by GENCI grant A0110807069.

■ REFERENCES

(1) Colvin, V. L.; Schlamp, M. C.; Allvlsatos, A. P. Light-Emitting Diodes Made from Cadmium Selenide Nanocrystals and a Semiconducting Polymer. *Nature* **1994**, *370*, 354−356.

(2) Fan, F.; Voznyy, O.; Sabatini, R. P.; Bicanic, K. T.; Adachi, M. M.; McBride, J. R.; et al. Continuous-Wave Lasing in Colloidal Quantum Dot Solids Enabled by Facet-Selective Epitaxy. *Nature* **2017**, *544*, 75−79.
(3) Han, K.; Yoon, S.; Chung, W. J. CdS and CdSe Quantum Dot-Embedded Silicate Glasses for LED Color Converter. *Int. J. Appl. Glass Sci.* **2015**, *6*, 103−108.
(4) Han, K.; Im, W. B.; Heo, J.; Chung, W. J. A Complete Inorganic Colour Converter Based on Quantum-Dot-Embedded Silicate Glasses for White Light-Emitting-Diodes. *Chem. Commun.* **2016**, *52*, 3564−3567.
(5) Guerreiro, P. T.; Ten, S.; Borrelli, N. F.; Butty, J.; Jabbour, G. E.; Peyghambarian, N. PbS Quantum-Dot Doped Glasses as Saturable Absorbers for Mode Locking of a Cr:Forsterite Laser. *Appl. Phys. Lett.* **1997**, *71*, 1596−1597.
(6) Reda, S. M. Synthesis and Optical Properties of CdS Quantum Dots Embedded in Silica Matrix Thin Films and Their Applications as Luminescent Solar Concentrators. *Acta Mater.* **2008**, *56*, 259−264.
(7) Xia, M.; Liu, C.; Zhao, Z.; Wang, J.; Lin, C.; Xu, Y.; et al. Surface Passivation of CdSe Quantum Dots in All Inorganic Amorphous Solid by Forming $Cd_{1-x}Zn_xSe$ Shell. *Sci Rep.* **2017**, *7*, No. 42359.
(8) Bell, G.; Filin, A. I.; Romanov, D. A.; Levis, R. J. Direct Growth of CdSe Semiconductor Quantum Dots in Glass Matrix by Femtosecond Laser Beam. *Appl. Phys. Lett.* **2016**, *108*, No. 063112.
(9) Lee, H.; Park, W. J.; Heo, J. Continuous-Wave Laser Irradiation to Form $Cd_{1-x}Zn_xSe$ Shell on CdSe QDs in Silicate Glasses. *J. Am. Ceram. Soc.* **2019**, *102*, 4555−4561.
(10) Xia, M.; Liu, C.; Xu, Y.; Zhao, X. Effect of Al_2O_3 on the Formation of Color Centers and CdSe/$Cd_{1-x}Zn_xSe$ Quantum Dots in SiO_2−Na_2O−ZnO Glasses. *J. Am. Ceram. Soc.* **2019**, *102*, 1726−1733.
(11) Xiong, Y.; Liu, C.; Wang, J.; Han, J.; Zhao, X. Near-Infrared Anti-Stokes Photoluminescence of PbS QDs Embedded in Glasses. *Opt. Express* **2017**, *25*, 6874−6882.
(12) Li, W.; Zhao, X.; Liu, C.; Coudert, F. X. Ab Initio Molecular Dynamics of CdSe Quantum-Dot-Doped Glasses. *J. Am. Chem. Soc.* **2020**, *142*, 3905−3912.
(13) Li, W.; Zhao, X.; Liu, C.; Coudert, F. X. Influence of Glass Composition on the Luminescence Mechanisms of CdSe Quantum-Dot-Doped Glasses. *J. Phys. Chem. C* **2021**, *125*, 18916−18926.
(14) Martínez, L.; Andrade, R.; Birgin, E. G.; Martinez, J. M. PACKMOL: a Package for Building Initial Configurations for Molecular Dynamics Simulations. *J. Comput. Chem.* **2009**, *30*, 2157−2164.
(15) Cormack, A. N.; Du, J. Molecular Dynamics Simulations of Soda-Lime-Silicate Glasses. *J. Non-Cryst. Solids* **2001**, *293*−*295*, 283−289.
(16) Pedone, A.; Malavasi, G.; Menziani, M. Z.; Cormack, A. N.; Segre, U. A New Self-Consistent Empirical Interatomic Potential Model for Oxides, Silicates and Silica-Based Glasses. *J. Phys. Chem. B* **2006**, *110*, 11780−11795.
(17) Smith, W.; Yong, C. W.; Rodger, P. M. DL_POLY: Application to Molecular Simulation. *Mol. Simul.* **2002**, *28*, 385−471.
(18) Li, W.; Li, N.; Liu, C.; Greaves, G. N.; Ong, W. J.; Zhao, X. Understanding the Atomic and Electronic Structures Origin of Defect Luminescence of CdSe Quantum Dots in Glass Matrix. *J. Am. Ceram. Soc.* **2019**, *102*, 5375−5385.
(19) Rabani, E. Structure and Electrostatic Properties of Passivated CdSe Nanocrystals. *J. Chem. Phys.* **2001**, *115*, 1493−1497.
(20) VandeVondele, J.; Krack, M.; Mohamed, F.; Parrinello, M.; Chassaing, T.; Hutter, J. Quickstep: Fast and Accurate Density Functional Calculations Using a Mixed Gaussian and Plane Waves Approach. *Comput. Phys. Commun.* **2005**, *167*, 103−128.
(21) Perdew, J. P.; Burke, K.; Ernzerhof, M. Generalized Gradient Approximation Made Simple. *Phys. Rev. Lett.* **1996**, *77*, 3865−3868.
(22) VandeVondele, J.; Hutter, J. Gaussian Basis Sets for Accurate Calculations on Molecular Systems in Gas and Condensed Phases. *J. Chem. Phys.* **2007**, *127*, No. 114105.
(23) Adamo, C.; Barone, V. Toward Reliable Density Functional Methods without Adjustable Parameters: The PBE0 model. *J. Chem. Phys.* **1999**, *110*, 6158−6170.
(24) Guidon, M.; Hutter, J.; VandeVondele, J. Auxiliary Density Matrix Methods for Hartree-Fock Exchange Calculations. *J. Chem. Theory Comput.* **2010**, *6*, 2348−2364.
(25) Tilocca, A.; de Leeuw, N. H. Structural and Electronic Properties of Modified Sodium and Soda-Lime Silicate Glasses by Car−Parrinello Molecular Dynamics. *J. Mater. Chem.* **2006**, *16*, 1950−1955.
(26) Demourgues, A.; Greaves, G. N.; Bilsborrow, R.; Baker, G.; Sery, A.; Speit, B. XAFS Study of CdSe Quantum Dots in a Silicate Glass. *Nucl. Instrum. Methods Phys. Res., Sect. B* **1995**, *97*, 166−168.
(27) Kottalanka, R. K.; Naktode, K.; Anga, S.; Nayek, H. P.; Panda, T. K. Heavier Alkaline Earth Metal Complexes with Phosphinoselenoic Amides: Evidence of Direct M-Se contact (M = Ca; Sr; Ba). *Dalton Trans.* **2013**, *42*, 4947−4956.
(28) Thomsen, R. M.; Skibsted, J.; Yue, Y. Z. The Charge-Balancing Role of Calcium and Alkali Ions in Per-Alkaline Aluminosilicate Glasses. *J. Phys. Chem. B* **2018**, *122*, 3184−3195.
(29) Pedone, A.; Gambuzzi, E.; Menziani, M. C. Unambiguous Description of the Oxygen Environment in Multicomponent Aluminosilicate Glasses from ^{17}O Solid State NMR Computational Spectroscopy. *J. Phys. Chem. C* **2012**, *116*, 14599−14609.

https://doi.org/10.1021/acs.jpcc.2c03917
J. Phys. Chem. C 2022, 126, 14283−14289